The effectiveness of three neural spike validation methods in setting appropriate spike boundaries

[1]Zuzana Rošťáková, [1]Roman Rosipal

[1]Institute of Measurement Science, Slovak Academy of Sciences, Bratislava, Slovakia
Email: zuzana.rostakova@savba.sk

Abstract. *Thresholding methods usually detect neural spikes or bursts of electrical pulses in a cortical electrophysiological signal. Due to the possibility of multiple threshold crossings representing the same spike, it is essential to set spike temporal boundaries to prevent double detection appropriately. We consider three spike validation methods and compare their performance on a set of simulated electrophysiological data mimicking the spiking activity of a neuron with different amounts of background noise. Since the results of one method rapidly deteriorated with decreasing signal-to-noise ratio, we formulate a modification leading to the algorithm's performance improvement.*

Keywords: spike validation, neural action potential, threshold crossing

1. Introduction

Neural spikes are short bursts of electrical pulses, or action potentials, through which neural cells communicate with each other (Fig. 1, right). They are usually recorded as the voltage changes by the thin glass or metal electrodes (pipettes) in the vicinity of a target neuron [1]. Among other approaches, neural spikes are detected by comparing the signal or its appropriate transformation with a fixed or adaptive (time-varying) threshold. Points with their amplitude over the positive threshold or under the negative threshold are denoted as spike candidates.

If one point crosses a threshold and is part of a spike, the neighbouring samples will also cross the threshold [2]. Many threshold crossings in a short period can therefore be viewed as the same event. Consequently, it is essential to determine spikes' start and end points correctly to avoid double detection. Performing this validation step may significantly reduce the number of false alarms, that is, spikes that are incorrectly detected [3].

This study aims to compare the performance of three spike validation methods in terms of their ability to detect the actual neural spike positions while minimising false alarms. However, in real-world data, the exact spike timing is unknown. Therefore, we used simulated data with known spike positions and different levels of background noise closely mirroring the properties of the real-world neural electrophysiological signal.

2. Data

Inspired by the work of Smith and Mtetwa [4], we simulated a five-second spiking activity of a neuron with the Poisson distribution of firing times and the sampling rate of 100 kHz. The spike shapes followed the realistic Naundorf model [5] with a spike duration of 4.44 ms and positive polarity. The number of spikes within this five-second long period varied between 316 and 334. The refractory period (Fig. 1, left) – a short interval after a spike during which a neuron is not able to fire – was set to a larger value (10 ms) to avoid too close or partially overlapped spikes.

The background noise included i) spike trains of seven neurons correlated with the spike train of the target neuron, and ii) the activity of other 100 neurons firing independently from the target neuron. The background noise amplitude was divided by 10 to avoid overlaying the target spikes. Finally, the signal was distorted by different amounts of Gaussian noise, resulting in six

levels of signal-to-noise ratio $SNR \in \{50, 35, 25, 10, 0, -5\}$ dB. For each SNR, we considered a set of 10 electrophysiological signals (Fig. 1, right).

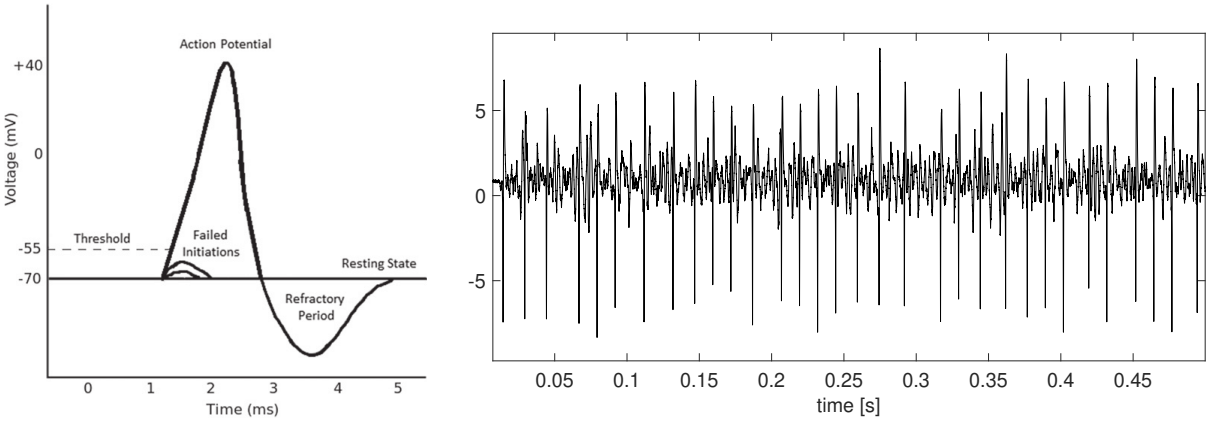

Fig. 1: *Left:* Schema of a neuron spike. Original image from [6]. *Right:* An example of a simulated electrophysiological signal with neural spikes and signal-to-noise ratio SNR = 35 dB.

3. Methods

In the first step, an adaptive threshold was set by the *AdaBandFlt* method [1], and an indicator vector for successful threshold crossings was computed for each simulated signal.

In the method of Wagenaar [3, 1], a candidate threshold crossing x represents a spike's centre only if it forms the highest peak of either polarity over the ± 1 ms time interval. Moreover, its amplitude should be at least two times higher than the amplitude of the second-highest peak with the same polarity on this interval (Condition 2). Finally, the distance between two consecutive spike centres should be at least θ_{refrac}, where θ_{refrac} represents the refractory period.

Toosi's method [2] sets the spike's center as the local minimum point to the right of the first threshold crossing if it does not occur within the previous spike's refractory period. Consequently, the spikes are aligned to their global minimum.

Nenadic [7] used a different approach. Time points where 0 changes to 1 or vice versa in the indicator vector represent starting and ending points of spikes. Then, the spike's centre candidate is computed as the mean between the corresponding starting and ending points. Consecutive candidate centre points x_i and x_{i+1} are analysed sequentially. If x_{i+1} and x_i are close to each other ($x_{i+1} - x_i \leq \theta_{merge}$), these two points represent the same spike with a high probability, and a new candidate centre point is computed $\left\lceil \frac{x_i + x_{i+1}}{2} \right\rceil$. If $x_{i+1} - x_i > \theta_{merge}$, but x_{i+1} lies within the refractory period of the i^{th} spike $\left(x_{i+1} - x_i < \theta_{refrac}\right)$, the candidate point x_{i+1} is discarded. Otherwise, x_i and x_{i+1} represent the centre of the i^{th} and $(i+1)^{th}$ spike, respectively.

After neural spike validation, we set the spike boundaries as $x \pm 2,22$ ms, where x represents the selected centre of a spike. Then, we computed the number of

i) correctly identified spikes (true positives, TP),
ii) undetected actual spikes (false negatives, FN),
iii) incorrectly detected spikes (false positives, FP), and
iv) the mean distance between detected and actual spikes starting points (mD)

for each method.

A spike was considered to be correctly identified if it overlapped at least 80% with one of the actual spikes. Then, the positive prediction rate (PPR), and sensitivity or recall (R) were evaluated by the following formulas

$$PPR = \frac{TP}{\#\text{ detected spikes}} = \frac{TP}{TP + FP} \qquad R = \frac{TP}{\#\text{ actual spikes}} = \frac{TP}{TP + FN}.$$

4. Results

All three methods successfully detected all generated spikes when data includes a small amount of Gaussian noise ($SNR = 50$ dB, Fig. 2).

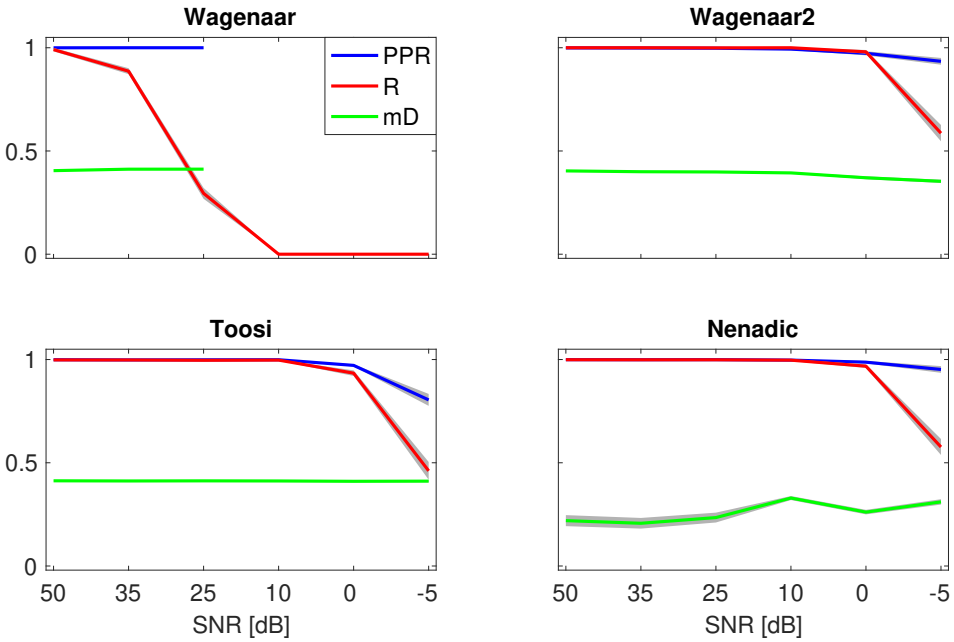

Fig. 2: The mean (solid line) $\pm$ standard deviation (shaded area) of positive prediction rate (*PPR*), recall (*R*) and the mean difference (*mD*) in starting points between actual spikes and spikes detected by the two versions of Wagenaar's method, Toosi's and Nenadic's approach.

The performance of Wagenaar's method deteriorated for $SNR \in \{25 \text{ dB}, 35 \text{ dB}\}$. Moreover, the algorithm was not able to detect any spike for $SNR \leq 10$ dB resulting in $R = 0$ and missing values of *PPR* and *mD* (Fig.2, top left). After a deeper inspection of Wagenaar's algorithm, we observed that the method's failure was caused by Condition 2, which was never met for data with a higher amount of noise. After removing Condition 2 from the algorithm (Wagenaar2), the method's performance improved. As depicted in Fig. 2 (top right), *PPR* and *R* for Wagenaaar2's and Nenadic's methods reached approximately the same values.

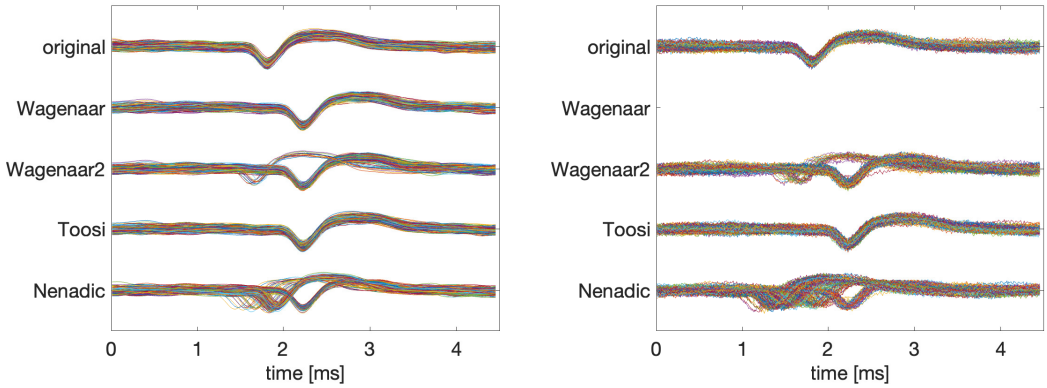

Fig. 3: Original simulated spikes with $SNR = 35$ dB (left) and $SNR = 10$ dB (right) and corresponding spikes detected by the two versions of Wagenaar's method, Toosi's and Nenadic's approach.

Methods of Toosi and Nenadic were able to detect almost all generated spikes, and their performance deteriorated only for $SNR \leq 0$ dB (Fig. 2, bottom). Nevertheless, this was expected because data with such a low *SNR* includes approximately the same amount of the target signal and noise.

Nenadic's algorithm achieved the lowest average temporal distance between the starting points of generated spikes and those correctly detected ($0.2 - 0.3$ ms, Fig. 2, bottom right), but at the cost of misaligned spikes characteristics (local minima and maxima, Fig. 3). On the other hand, constant $mD \approx 0.41$ ms was observed for all levels of *SNR* in Toosi's approach due to spike alignment to their global minima. Although Wagenaar's approach does not align the spikes a priori, its *mD* values were similar to Toosi's results, and the detected spikes were also aligned to the local minimum. However, as depicted in Fig. 3, the spikes alignment disappears after removing Condition 2 (Wagenaar2) for $SNR \leq 35$ dB.

5. Discussion and Conclusions

In this article, we compared the ability of three spike validation methods to identify spikes in simulated neural electrophysiological data. Wagenaar's method was unable to detect spikes when more noise was present because any candidate spike satisfied the condition of having the global peak amplitude at least twice as high as the second-highest peak of the same polarity. After removing this condition from the algorithm, the method's performance increased and was comparable to Toosi's and Nenadic's methods.

Nenadic's method sets the starting points of detected spikes closest to the generated spikes but at the cost of spikes misalignment. Spike validation is usually followed by spike clustering in order to detect dominant spike patterns. When using Nenadic's approach, we recommend aligning spikes before clustering because misalignment may result in many spurious or outlier clusters. On the other hand, this alignment step is not necessary when considering Toosi's algorithm. It's only required to realize that Toosi's spikes start a bit earlier than the actual spikes. Therefore we can conclude that Toosi's and Nenadic's methods can be used for spike validation.

Nevertheless, in this study we examined a specific case with spikes following the same amplitude and having a relatively long refractory period. Therefore, further analysis of simulated data with spikes following varying amplitudes or shorter refractory periods is needed.

Acknowledgements

This research was supported by the grant APVV-21-0105 and by the VEGA grant 2/0057/22.

References

[1] Biffi, E., Ghezzi, D., Pedrocchi, A., Ferrigno, G. (2010). Development and validation of a spike detection and classification algorithm aimed at implementation on hardware devices. *Computational Intelligence and Neuroscience* 2010(659050).

[2] Toosi, R., Akhaee, M., Dehaqani, M.-R. (2021). An automatic spike sorting algorithm based on adaptive spike detection and a mixture of skew-t distributions. *Scientific Reports* 11(13925).

[3] Wagenaar, D., DeMarse, T., Potter, S. (2005). MeaBench: a toolset for multi-electrode data acquisition and on-line analysis. In: *2nd International IEEE EMBS Conference on Neural Engineering, 2005.* pp. 518–521.

[4] Smith, L. S., Mtetwa, N. (2007). A tool for synthesizing spike trains with realistic interference. *Journal of Neuroscience Methods* 159(1), 170–180.

[5] Naundorf, B., Wolf, F., Volgushev, M. (2006). Unique features of action potential initiation in cortical neurons. *Nature* 440, 1060–1063.

[6] Ajayan, A., James, A. (2021). Edge to quantum: Hybrid quantum-spiking neural network image classifier. *Neuromorphic Computing and Engineering* 1(024001).

[7] Nenadic, Z., Burdick, J. (2005). Spike detection using the continuous wavelet transform. *IEEE Transactions on Biomedical Engineering* 52(1), 74–87.